

# Design, analysis and testing of a piezoelectric flex transducer for harvesting bio-kinetic energy

A Daniels<sup>1</sup>, M Zhu<sup>2\*</sup> and A Tiwari<sup>1</sup>

<sup>1</sup> Department of Manufacturing and Materials, Cranfield University, Bedfordshire, MK43 0AL, UK.

<sup>2</sup> College of Engineering, Mathematics and physical sciences, Exeter University, Exeter, EX4 4QF, UK.

\*E-mail: m.zhu@exeter.ac.uk

**Abstract.** The increasing prevalence of low power consuming electronics brings greater potential to mobile energy harvesting devices as a possible power source. A new piezoelectric energy harvesting device, called the piezoelectric flex transducer (PFT), is presented and developed. A Finite Element Model (FEM) was developed to design and analyse the PFT. The PFT consists of a piezoelectric element sandwiched between substrate layers and metal endcaps that are able to amplify the axial force on the piezoelectric element. Based on the concept of the Cymbal transducer, the PFT can withstand higher forces, was retrofitted into a shoe and used to power a wireless sensor module whilst the subject with a body weight of 760N was wearing the shoe and ran at 3.1mph (1.4HZ on shoe), the PFT produced an average maximum power of 2.5mW (over 2M $\Omega$  load).

## 1. Introduction

Based on the concept of the cymbal device [1], the piezoelectric flex transducer (PFT) is composed of top and bottom endcaps with a central piezoelectric element. Unlike the cymbal, the PFT has additional substrate layers which enable the device to be scaled up and therefore withstand forces of up to 1kN. This is because the substrate layers can increase the adhesion contact area, therefore reducing delamination risks. The PFT has rectangular shape for an improved packing factor.

The value of mobile energy harvesting is in the benefits of autonomy, reduced monetary and environmental costs. The power output of bio-kinetic mobile energy harvesting devices is an important factor for applications so we take a system level design approach to increase the power output and decrease power consumption at every level. This paper presents the design, analysis, fabrication and testing of the PFT. The energy generated by the PFT in gait (bio-kinetic energy) when retrofitted into a shoe was demonstrated to power a custom developed wireless sensor module [2].

## 2. Piezoelectric Flex Transducer (PFT)

The PFT consists of a piezoelectric element sandwiched between substrate layers and two metal endcaps, shown in figure 1. The stainless steel endcaps have two main functions: 1) to amplify and redirect the downward applied mechanical force to a horizontal force so that the majority of the

\* Author to whom any correspondence should be addressed



available force acts to stretch piezo-element horizontally, the converse action happens when the force is removed and the PFT tends back to a physically neutral state, and 2) to suspend the piezo-element and substrate so that they can actuate more freely, generally speaking a higher straining corresponds to a higher charge produced.

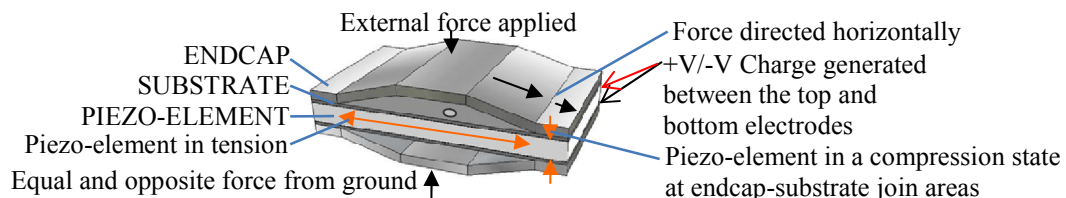


**Figure 1.** Function of the PFT when a downward compressive force is applied.

The endcaps and substrates were made from stainless steel by Rye-Guard Ltd (Bedfordshire, UK), whereby sheet metal bending was used to form the endcaps. The piezoelectric elements with silver fired electrodes were tailor-made from DL-35HD material by DeL Piezo Specialties, LLC (Florida, USA). Following the welding together of the substrates and endcaps by The Welding Institute (Cranfield University, UK) surfaces were textured and a 3M Scotch-Weld™ DP-460 structural adhesive was spread on the substrate-piezoelectric interfaces and baked (approx. 50 minutes at 90°C). A clamp was used to hold the device together whilst baking. Wire connections to the electrodes were made through pre-drilled 2mm diameter holes in the substrates. Two types of endcap-substrate weld methods were experimented with; laser and resistance spot welding, both performed similarly, however, fatigue analysis was not performed.

### 3. Design analysis

ANSYS (Version 13), a multi-physics finite element analysis (FEA) software package, was used to develop a coupled piezoelectric-circuit finite element model (CPC-FEM) of the PFT for design analyses. The CPC-FEM is comprised of the 3-dimensional structure of the PFT with a load resistor connected in parallel between the 'electrodes' of the piezo-element, shown in figure 2. Running a harmonic analysis the CPC-FEM has the ability to calculate the electrical output of the PFT whilst it was subjected to an external force excitation, such possible outputs were: the peak voltage, current and power. Static analyses were also carried out to establish the mechanical stress of the PFT.

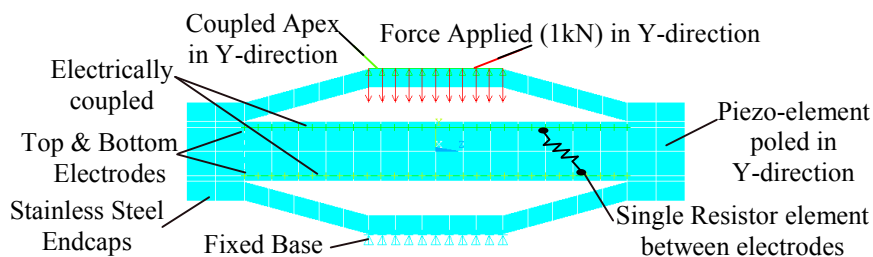


**Figure 2.** PFT as seen in CPC-FEM with boundary conditions and electrical resistor connected in parallel between top and bottom electrically coupled surfaces.

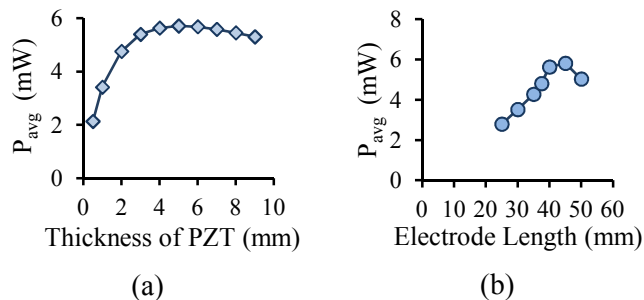
The element type used for the piezo-element was SOLID226. SOLID226 is a couple-field element type, capable of analysing piezoelectric structural and electrical performance. Secondly, SOLID95 was used for the endcaps. Finally, CIRCU94 was used for the resistor element connected between the piezo-element electrically coupled node surfaces. The PFT was modelled with the lower endcap fixed and a universally distributed load applied to the upper surface of the top endcap. The force applied to the top endcap was 1kN, which was an approximation of what an average male might exert on the ground whilst in gait. Because electrode and adhesion layers were very thin, they were ignored in the model. Stainless steel input properties used in the CPC-FEM were: Young's modulus 193GPa, density 8030 kg m<sup>-3</sup> and Poisson's ratio 0.24.

**Table 1.** Dimensions of PFT in CPC-FEM and in experiment.

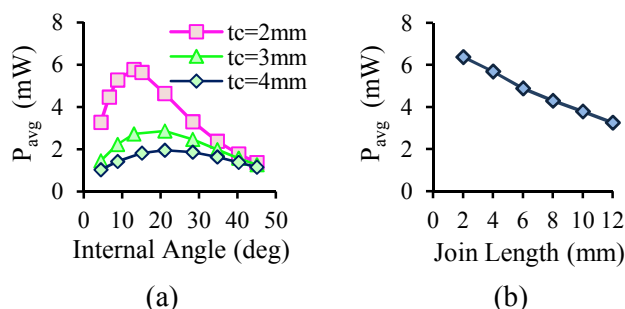
Total Length	D	52mm	Endcap Thickness	$t_c$	2mm
Total Width	$D_w$	30mm	Join Length	J	6mm
Piezo Thickness	$t_p$	4mm	Cavity Length	$D_c$	40mm
Apex Length	$D_a$	14mm	Angle of the Endcap	$\Theta$	$8.75^\circ$

**Table 2.** Piezoelectric material properties used in CPC-FEM.

Piezoelectric Material: DeL Piezo DL-53HD											
Elastic Compliance ( $\times 10^{-12} \text{ m}^2 \text{ N}^{-1}$ )				Piezoelectric strain constants ( $\times 10^{-12} \text{ m V}^{-1}$ )		Relative Dielectric Constant (constant stress)		Density ( $\text{Kg m}^{-3}$ )		Piezoelectric Coupling Coefficient	
$s_{11}$	15.1	$s_{33}$	24.8	$d_{15}$	810	$\epsilon_{11}^T$	3550	$\rho$	7900	$k_{31}$	0.4
$s_{12}$	-4.5	$s_{44}$	37.1	$d_{31}$	-300	$\epsilon_{33}^T$	3850				
$s_{13}$	-9.4	$s_{66}$	39.2	$d_{33}$	680						
										Q	20

**Figure 3.** (a) and (b) Power output of the PFT for different piezo-element thicknesses and different electrode lengths along piezo-element, respectively. The PFT was subject to a 1kN force at 2Hz. For each point on the graphs the optimal resistance was used.

In figure 3 (a) the power output increased with an increase in piezo-thickness for a PFT under a 1kN force load at 2Hz. When the thickness of the piezo-element was increased, the capacitance decreased and the internal resistance increased. This resulted in a variation of voltage and current produced, where by an increased thickness caused an increased voltage but a decreased current. When the electrode area coverage was varied across the piezo-element top and bottom region, figure 3 (b), results showed that the most effective coverage, 40mm, was one that excluded the clamped region (join length) of the piezo-element. Piezoelectric material in the join length was effectively clamped and thus contributed negligible charge when the PFT was in use. It was thought the reason why the partial electrode fared better was that if the partial electrode PFT produced the same charge as a full electrode PFT but with a reduced capacitance—due to its smaller electrodes—it must have an increased voltage and thus also an increased power output.

**Figure 4.** (a) and (b) Power output for different endcap thickness and internal angles (10M $\Omega$ ), and endcap-substrate join length (8M $\Omega$ ), respectively. PFT subject to a 1kN force at 2Hz. Internal angle remained constant when changing join length.

Enhanced PFT power outputs were found with the following: reduced endcap thickness led to less energy waste through unneeded bulk, figure 4 (a), though not shown here this was similar with

substrate thickness. Reduced endcap internal angle gave rise to more horizontal force along the piezo-element due to leverage effects, figure 4 (a) and finally reduced joint length decreased wasteful clamping of the piezoelectric element, figure 4 (b). Though not shown here the current and voltage showed a similar trend to power output when varying the endcap dimensions as in figure 4 (a) and (b). This was expected as the internal properties of the piezo-element remained constant, it was only the force applied to the piezo-element that changed. Factors that limited the choice of the joint length and substrate were fabrication difficulty. The main limiting factor of choosing the piezo-element thickness was the internal resistance i.e. very thick piezo-elements had a high internal resistance, which was undesired. Finally mechanical stress was the limiting factor when choosing the thickness and internal angle of the endcaps. Following that the stainless steel used had a Yield Strength of 125MPa (already with safety factor of 2 applied) for chosen dimensions see table 1. Though not shown here four metallic materials were considered for the endcaps; aluminium, titanium, stainless steel and copper alloy. It was found that making the endcaps thinner had a greater effect on power output than having a reduced stiffness, so possessing a high Yield Strength was important in order to get the thinnest possible endcap. Titanium performed best however, a compromise based on cost meant that stainless steel was used. Stainless steel was also used to make the substrate for similar reasons. Piezoelectric material selection was based on guidelines set out in previous works [3] with the additional compromise of availability.

#### 4. Shoe Application Demonstration



**Figure 5.** Testing of PFT in a shoe using a treadmill. PFT retrofitted into shoe with extra steel plate and held in place with nylon strap.

The PFT was retrofitted into a shoe and connected by wire to a wireless module [2]. The wireless module housed three sensors to measure acceleration, light and temperature. The measurement data were then wirelessly transmitted to a base-station equipped with a JN5148 wireless microcontroller (compliant with IEEE 802.15.4 protocol at 2.4GHz frequency). The transceiver was linked via USB with a laptop for further analysis.

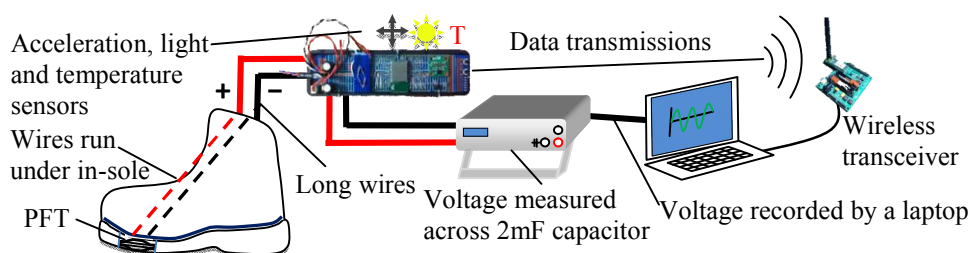


**Figure 6.** Testing set-up of PFT retrofitted in a shoe and the energy generated was used to power a wireless sensor module whilst the subject ran on a treadmill.

During the test the voltage across a capacitor in the wireless module was measured using a multi-meter. This capacitor was charged by electrical energy from the PFT and the energy was also used to power the module. Therefore, its voltage level gave an indication of what function the wireless module was carrying out.

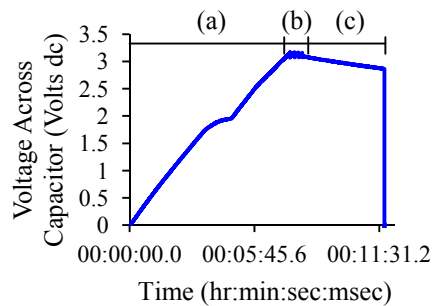


**Figure 7.** Voltage across 2mF capacitor connected to wireless module powered by PFT when subjected to approximately 760N at 1.4Hz whilst in shoe: (a) cold start, (b) data transmissions and (c) capacitor discharge; subject stopped running.

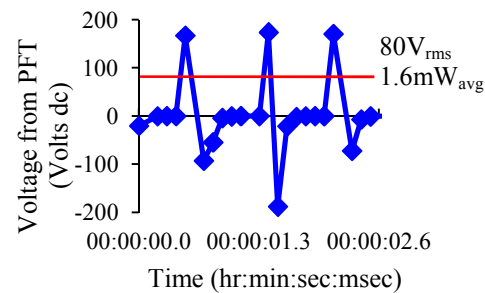


**Figure 8.** Voltage measured across a 4MΩ resistor connected in parallel to the PFT (4MΩ replacing the resistive load previously supplied by wireless module). When subjected to approximately 760N at 1.4Hz whilst in shoe.

Figure 7 shows the voltage across the 2mF capacitor connected to a wireless module with respect to time. The initial cold start time of 7minutes, zone (a), meant that the subject had to run for 7minutes continuously (exerting a force of 760N at 1.4Hz on the PFT) to initially charge the capacitor. As soon as the capacitor reached wireless module functioning threshold-voltage,  $\sim 3.2\text{V}$ , sensor reading and transmission of the data were performed, zone (b). The wireless module warm start is represented in the graph by the ascending voltage from  $\sim 3.08\text{V}$  to  $\sim 3.2\text{V}$  when the capacitor is energy recovering between module sensor readings and data transmission. The energy level provided by the subject running was enough to provide a short warm start of approximately 10s. The power consumed by the wireless module during sensor reading and data transmission is represented as a voltage drop from  $\sim 3.2\text{V}$  to  $\sim 3.08\text{V}$ . When the subject stopped running the voltage dropped to zero, zone (c). The data from each sensor was received at the laptop base station and recorded. The voltage fluctuations in Figure 8 correspond to foot strikes, where a 4MΩ resistor was connected to the PFT as an external resistor load replacing the wireless module in order to measure the power produced by the PFT directly. Though not shown here, when tested over a resistance range of 1-10MΩ (1MΩ intervals) the PFT produced a maximum power of  $2.5\text{mW}_{\text{avg}}$  over 2MΩ ( $71\text{V}_{\text{rms}}$   $36\mu\text{A}_{\text{rms}}$ ).

## 5. Conclusion

This paper used a coupled piezoelectric-circuit finite element model (CPC-FEM) to design and analyse the novel piezoelectric flex transducer's (PFTs) performance with focus on some key dimensional parameters. The PFT was fabricated, retrofitted into a shoe and the energy generated was used to power a wireless sensor module whilst the subject wearing the shoes ran at approximately 3.1mph.

## Acknowledgments

The authors gratefully acknowledge support from SmartWater: "Smart Sensor Network with energy harvesting for real time monitoring in urban water infrastructure" (FP7-People-2-12-IRSES project, EC318985) and to Wojciech Suder at the Welding Institute (Cranfield University) for welding the PFT.

## 6. References

- [1] Kim H, Priya S, Stephanou H, Uchino K 2007 *IEEE. T. Ultrason. Ferr* **54** (9) 1851-1858
- [2] Giuliano A, Marsic V, Zhu M 2012 *IEEE. Int. Conf. iThings* 681-684
- [3] Daniels A, Zhu M, Tiwari A 2013 *IEEE. T. Ultrason. Ferr* (Accepted)